A simple and unified algorithm to solve fluid phase equilibria using either the gamma-phi or the phi-phi approach for binary and ternary mixtures

Romain PRIVAT[*,a], Jean-Noël JAUBERT[a] and Yannick PRIVAT[b]

[a] École Nationale Supérieure des Industries Chimiques, Université de Lorraine, Laboratoire Réactions et Génie des Procédés - UPR 3349, 1 rue Grandville, BP 20451, Nancy cedex 9, France.

[b] ENS Cachan, antenne de Bretagne - avenue Robert Schumann, 35170 Bruz, France.

[*] *Corresponding author.* E-mail: romain.privat@univ-lorraine.fr. Telephone number: (+33)383175128. Fax number: (+33)383175152.

Abstract

A new algorithm is proposed for calculating phase equilibria in binary systems at a fixed temperature and pressure. This algorithm is then extended to ternary systems (in which case, the mole fraction of one constituent in a given phase must be fixed in order to satisfy the Gibbs' phase rule). The algorithm has the advantage of being very simple to implement and insensitive to the procedure used to initialize the unknowns. Most significantly, the algorithm allows the same solution procedure to be used regardless of the thermodynamic approach considered ($\gamma - \varphi$ or $\varphi - \varphi$), the type of phase equilibrium (VLE, LLE etc.) and the existence of singularities (azeotropy, criticality and so on).

Keywords: Phase-equilibrium calculation, algorithm, binary mixtures, ternary mixtures, phi-phi, gamma-phi.

1 Introduction

Several industrially important chemical applications such as single- and multi stage processes (including flash, distillation, absorption, extraction etc.) bring two fluid phases into contact (e.g., two liquid phases or a liquid phase and a vapor phase). Simulation and optimization of these processes require that the properties of the equilibrium states be calculated, mainly, the temperature T, the pressure P and the compositions of the coexisting phases. Robust and efficient algorithms for phase-equilibrium calculations are therefore needed. The Gibbs' phase rule states that calculating two-phase equilibrium in a **binary system** requires **two** intensive and independent process variables to be specified which are typically chosen from T, P, x_i' (the mole fraction of component i in the first phase) and x_i'' (the mole fraction of component i in the second phase). The phase-equilibrium problem then consists of solving a set of two equilibrium equations with respect to two unknowns:

$$\begin{cases} \mu_1'(T,P,x_1') &= \mu_1''(T,P,x_1'') \\ \mu_2'(T,P,x_1') &= \mu_2''(T,P,x_1'') \end{cases} \tag{1}$$

where μ_i denotes the chemical potential of component i in a given phase. The superscripts $'$ and $''$ denote the first and second equilibrium phases respectively. The procedure for solving the two equilibrium equations is strongly related to (i) the choice of the two specified variables and to (ii) the nature of the equilibrium (liquid-liquid or liquid-vapor) involved. There are six possible combinations of two variables among the four aforementioned ones (T, P, x_i' and x_i''). Four of them are often acknowledged to be of practical interest since they can be easily generalized to p-component systems with $p > 2$. This is why many papers and textbooks propose solution procedures for only the following four cases [1–3]:

- Calculation of x_i' (or x_i'') and P, given x_i'' (or x_i') and T. For vapor-liquid equilibrium (VLE), these kinds of calculations are called *bubble-point pressure* and *dew-point pressure calculations*.
- Calculation of x_i' (or x_i'') and T, given x_i'' (or x_i') and P. For VLE, these kinds of calculations are called *bubble-point temperature* and *dew-point temperature calculations*.

The two remaining combinations which are scarcely - if ever - considered are:

- Calculation of T and P, given x_i' and x_i''.

- Calculation of x_i' and x_i'', given T and P.

The first calculation which requires that the mole fractions in the two phases be specified, is clearly of no practical interest. Indeed, in this case, temperature and pressure which are certainly the easiest process variables to work with, are not specified but become accessible after solving the phase-equilibrium problem.
The second combination (where the variables T and P are specified) appears to be particularly convenient. To give an example, calculation of the complete isothermal or isobaric binary phase diagrams is straightforward using an algorithm with T and P as specified variables, as opposed to an algorithm using x_i' and x_i'' as specified variables.

At this point, it is important to highlight that calculating the compositions of two phases in equilibrium at a fixed T and P differs notably from the classical (P,T)-flash calculation. Indeed, calculating x_i' and x_i'' at given T and P only involves **phase variables** (T, P and the mole fractions in the two phases) but does not involve any **overall variable** (the proportion of the phases, overall mole fractions etc.). In contrast, a flash algorithm involves both phase variables and overall variables.
More specifically:

- in a (P,T)-flash algorithm, the variables T and P are specified along with the overall composition (by comparison, the calculation of x_i' and x_i'' at a given T and P only requires T and P to be specified),

- in a (P,T)-flash algorithm, the two phase-equilibrium equations are coupled with material balances (whereas the calculation of x_i' and x_i'' at a given T and P only involves the phase-equilibrium equations),

- in a (P,T)-flash algorithm, the unknowns are x_i' and x_i'' as well as τ, the molar proportion of a given phase (whereas for the calculation of x_i' and x_i'' at a given T and P, x_i' and x_i'' are the sole unknowns).

- At a given T and P, depending on the overall composition, a (P,T)-flash algorithm can indicate whether the system is made up of a single phase (molar proportions of the phases $= 0$ or 1) or two phases (molar proportions $\in]0\ ;\ 1[$). The calculation of x_i' and x_i'' is then

only performed in the latter case.

In summary, a (P,T)-flash algorithm and the calculation of x_i' and x_i'' at a given T and P do not involve the same input variables, the same unknowns and the same set of equations to solve.
In addition, contrary to a (P,T)-flash algorithm, the calculation of x_i' and x_i'' at a given T and P allows uncoupling the phase-equilibrium problem and the resolution of the mass-balance equations which may have two interests:

- the dimension of the system of equations to solve becomes smaller which may facilitate its resolution;
- the phase-equilibrium problem takes the advantageous form of a pseudo-linear system, as will be proved in the next sections.

In this paper, a new algorithm is proposed to calculate phase equilibria in binary systems at a specified T and P. As will be shown, the algorithm can be used either with the $\gamma - \varphi$ or the $\varphi - \varphi$ approach and allows VLE or LLE (liquid-liquid equilibria) to be calculated as well. This procedure is considered to be *universal*, as it unifies the various approaches and kinds of fluid-phase equilibrium calculations. The great simplicity of the algorithm facilitates easy implementation. The algorithm can be used to calculate complex phase diagrams exhibiting azeotropy or criticality, and is thus intended for audiences in academic or industrial environments who use phase-equilibrium thermodynamics as a tool and wish to have at their disposal a unique algorithm to perform either VLE or LLE calculations.
Therefore, the algorithm can be used indifferently to model, e.g., a distillation column, a stripping process, a liquid-liquid extraction or any separation unit involving fluid-fluid phase equilibria.

The final section of the paper shows how this algorithm can be simply extended to ternary systems by specifying a third variable.

2 General formalism of the two-phase equilibrium problem in binary systems at specified temperature and pressure

2.1 The $\gamma - \varphi$ approach

In the present case, a liquid-activity-coefficient model (also known as molar excess Gibbs energy model) is used to evaluate the thermodynamic properties of the liquid phase. An equation of state (EoS) is used for the gaseous phase.

- For a binary system in liquid-liquid equilibrium at a fixed temperature T and pressure P, Eq. (1) may be written as follows:

$$\begin{cases} x_1' \cdot \gamma_1(x_1') &= x_1'' \cdot \gamma_1(x_1'') \\ (1 - x_1') \cdot \gamma_2(x_1') &= (1 - x_1'') \cdot \gamma_2(x_1'') \end{cases} \tag{2}$$

  where x_1' and x_1'' are the mole fractions of component 1 in each of the two liquid phases in equilibrium and γ_i denotes the activity coefficient of component i in a liquid phase. γ_i is classically derived from an excess Gibbs energy model, such that: $RT \ln \gamma_i = (\partial G^E / \partial n_i)_{T,P,n_{j \neq i}}$ where G^E is the total molar Gibbs energy of the liquid phase and n_i, the amount of component i in the liquid phase. These kinds of model are pressure-independent so that, the liquid-activity coefficients depend only on the mole fractions and the temperature. For the sake of clarity, only the two unknowns x_1' and x_1'' in the phase-equilibrium problem at fixed T and P appear within parentheses, in Eq. (2).

- For liquid-vapor equilibrium at a fixed temperature T and pressure P, Eq. (1) is equivalent to:

$$\begin{cases} P \cdot y_1 \cdot C_1(y_1) &= P_1^{\text{sat}} \cdot x_1 \cdot \gamma_1(x_1) \\ P \cdot (1 - y_1) \cdot C_2(y_1) &= P_2^{\text{sat}} \cdot (1 - x_1) \cdot \gamma_2(x_1) \end{cases} \tag{3}$$

  where x_1 and y_1 are the mole fractions of component 1 in the liquid and vapor phases, respectively; P_i^{sat} is the vapor pressure of the pure component i; the coefficient C_i is defined as:

$$C_i(y_1) = \frac{\hat{\varphi}_i^{\text{gas}}(y_1)}{\varphi_i^{\text{sat}}} \cdot F_{P,i} \tag{4}$$

  where $\hat{\varphi}_i^{\text{gas}}$ is the fugacity coefficient of component i in the gas phase, φ_i^{sat} is the fugacity coefficient of pure i at its vapor pressure at temperature T and $F_{P,i}$ is the classical Poynting

correction factor for component i at T and P (often set to 1 at low to moderate pressures). Eq. (3) can be alternatively written as follows:

$$\left\{\begin{array}{rcl} x_1 \cdot \gamma_1(x_1) & = & y_1 \cdot \left[P \cdot C_1(y_1)/P_1^{\text{sat}}\right] \\ (1-x_1) \cdot \gamma_2(x_1) & = & (1-y_1) \cdot \left[P \cdot C_2(y_1)/P_2^{\text{sat}}\right] \end{array}\right. \tag{5}$$

As before, only the two unknowns (x_1 and y_1) in the phase-equilibrium problem at a fixed T and P appear within parentheses in Eq. (5).

2.2 The $\varphi - \varphi$ approach

This approach requires the use of a pressure-explicit EoS to model both phases in equilibrium. The method offers the undeniable advantage of a unique formalism for liquid-liquid, liquid-vapor and more generally fluid-fluid phase equilibria. Eq. (1) is then written as follows:

$$\left\{\begin{array}{rcl} x_1' \cdot \hat{\varphi}_1' & = & x_1'' \cdot \hat{\varphi}_1'' \\ (1-x_1') \cdot \hat{\varphi}_2' & = & (1-x_1'') \cdot \hat{\varphi}_2'' \end{array}\right. \tag{6}$$

where x_1' and x_1'' are the mole fractions of component 1 in the two fluid phases in equilibrium; $\hat{\varphi}_i'$ and $\hat{\varphi}_i''$ denote the fugacity coefficients of component i in each fluid phase.

For a binary system, the pressure-explicit EoS expresses the pressure of a phase as a function of the temperature T of the phase, the mole fraction z_1 of component 1 and the molar volume v of the phase. Henceforth, the pressure-explicit EoS will be denoted by the function: $P_{\text{EoS}}(T, v, z_1)$. Expressions for the fugacity coefficients are derived from the EoS and are thus natural functions of the variables T, v and z_1: $\hat{\varphi}_i(T, v, z_1)$.

Consequently, the fugacity coefficients $\hat{\varphi}_i'$ and $\hat{\varphi}_i''$ of component i in the two phases in equilibrium are accessible at a fixed temperature T_0 and pressure P_0, provided that the molar volumes (v' and v'') and the mole fractions of component 1 (x_1' and x_1'') are known: $\hat{\varphi}_i' = \hat{\varphi}_i(T_0, v', x_1')$ and $\hat{\varphi}_i'' = \hat{\varphi}_i(T_0, v'', x_1'')$. The molar volume of a fluid phase can be calculated by solving the EoS, given the temperature, the pressure and the composition of the phase. Therefore, at fixed T_0 and P_0, the unknowns v' and v'' are obtained by solving the two equations: $P_0 = P_{\text{EoS}}(T_0, v', x_1')$ and $P_0 = P_{\text{EoS}}(T_0, v'', x_1'')$ (by assuming known values of mole fractions x_1' and x_1'').

Finally, the phase-equilibrium problem at a fixed temperature T_0 and pressure P_0 using a $\varphi - \varphi$ approach, is reduced to solving a set of four equations with respect to four unknowns (v', x_1', v'',

x_1''):

$$\left\{\begin{array}{rcl} x_1' \cdot \hat{\varphi}_1(v', x_1') & = & x_1'' \cdot \hat{\varphi}_1(v'', x_1'') \\ (1 - x_1') \cdot \hat{\varphi}_2(v', x_1') & = & (1 - x_1'') \cdot \hat{\varphi}_2(v'', x_1'') \\ P_0 & = & P_{\mathrm{EoS}}(v', x_1') \\ P_0 & = & P_{\mathrm{EoS}}(v'', x_1'') \end{array}\right. \tag{7}$$

Once again, only the unknowns in the problem appear within parentheses.

2.3 Writing of the phase-equilibrium problem using a unique formalism

Eqs. (2), (5) and (6) can be written in the following unified form:

$$\left\{\begin{array}{rcl} x_1' \cdot F_1' & = & x_1'' \cdot F_1'' \\ (1 - x_1') \cdot F_2' & = & (1 - x_1'') \cdot F_2'' \end{array}\right. \tag{8}$$

Expressions for the functions F_1', F_1'', F_2' and F_2'' are given in Table 1 and are selected based on the chosen approach and the kind of phase-equilibrium calculation (VLE, LLE ...) being considered.

3 Derivation of a unique algorithm for phase-equilibrium calculation in binary systems at a fixed temperature and pressure

3.1 General solution procedure

Eq. (8) can be equivalently written as:

$$\left\{\begin{array}{rcrcl} x_1' \cdot F_1' & - & x_1'' \cdot F_1'' & = & 0 \\ -x_1' \cdot F_2' & + & x_1'' \cdot F_2'' & = & F_2'' - F_2' \end{array}\right. \tag{9}$$

Such a system is highly nonlinear and the coefficients F_1', F_1'', F_2' and F_2'' depend on x_1' and x_1''. Using matrix notations, Eq. (9) can be alternatively written as:

$$\underbrace{\begin{pmatrix} F_1' & -F_1'' \\ -F_2' & F_2'' \end{pmatrix}}_{\mathbf{A}(\mathbf{X})} \underbrace{\begin{pmatrix} x_1' \\ x_1'' \end{pmatrix}}_{\mathbf{X}} = \underbrace{\begin{pmatrix} 0 \\ F_2'' - F_2' \end{pmatrix}}_{\mathbf{B}(\mathbf{X})} \tag{10}$$

or equivalently, providing matrix $\mathbf{A}$ can be inverted:

$$\mathbf{X} = [\mathbf{A}(\mathbf{X})]^{-\mathbf{1}} \ \mathbf{B}(\mathbf{X}) \tag{11}$$

with:

$$\mathbf{A^{-1}} = \frac{1}{\det(\mathbf{A})} \begin{pmatrix} F_2'' & F_1'' \\ F_2' & F_1' \end{pmatrix} \tag{12}$$

Consequently, the values of the mole fractions x_1' and x_1'' at iteration $(k+1)$ can be deduced from the values of the quantities F_1', F_1'', F_2' and F_2'' at iteration k as follows:

$$\boxed{\begin{cases} {x_1'}^{(k+1)} &= \left[\dfrac{F_1''\ (F_2'' - F_2')}{F_1'\ F_2'' - F_1''\ F_2'}\right]^{(k)} \\ {x_1''}^{(k+1)} &= \left[\dfrac{F_1'\ (F_2'' - F_2')}{F_1'\ F_2'' - F_1''\ F_2'}\right]^{(k)} = {x_1'}^{(k+1)} \left(\dfrac{F_1'}{F_1''}\right)^{(k)} \end{cases}} \tag{13}$$

This iterative scheme represents the main result of this paper and is actually an application of the classical direct-substitution method to the two-phase equilibrium problem. Algorithms based on the following procedure can be used to calculate phase equilibria:

1. Provide initial estimates for the unknowns x_1' and x_1''. Set the iteration counter to $k = 0$.

2. Calculate the coefficients F_1', F_2', F_1'' and F_2'' for the current iteration k.

3. Define a convergence criterion δ as follows:

$$\delta = \left[\left|x_1'' F_1'' - x_1' F_1'\right| + \left|(1 - x_1'') F_2'' - (1 - x_1') F_2'\right|\right]^{(k)} \tag{14}$$

   If δ is low enough, then convergence is reached and the procedure is terminated.

4. Update the unknowns x_1' and x_1'' using Eq. (13); update the iteration counter to $(k = k+1)$ and return to step 2.

The subsequent sections illustrate the efficiency of the iterative scheme and discuss its range of applicability.

3.2 Preliminary remarks regarding the convergence of the procedure for the general solution

Next sections are intended to convince the reader that the proposed formulation of the two-phase equilibrium problem coupled with the solution procedure can deal with complex scenarios efficiently and has a wide range of applicability. However, it is clearly not possible to guaranty convergence in all cases. It is indeed well known that fixed-point methods - including direct-substitution methods - can potentially fail due to the existence of diverging sequences that depend

on the nature of the equation to solve and the initial guesses to the solution. In this regard, Lucia et al. have pointed out that even chaotic and periodic behaviors can be exhibited by fixed-point methods [4], thus emphasizing the complexity of a convergence study.

Therefore, it seems very difficult, if not impossible, to determine a priori for which cases, the method will converge or diverge. In Appendices A and B, some mathematical results on the convergence of fixed-point methods are applied to two-phase equilibrium problems; a general methodology for studying failed cases is also provided.

3.3 Numerical example 1: calculation of liquid-liquid phase equilibrium using an activity-coefficient model

In order to illustrate the simplicity of the iterative scheme given by Eq. (13), let us calculate the compositions x_1' and x_1'' of two liquid phases in equilibrium at $T = 300\ K$ for a fictitious binary system (1) + (2), using the $\gamma - \varphi$ approach. The non-ideality of the liquid phase is accounted for by a Van-Laar type activity-coefficient model [3]:

$$g^E(x_1) = \frac{A_{12}A_{21}x_1x_2}{A_{12}x_1 + A_{21}x_2}, \qquad \text{with} \begin{cases} x_2 = 1 - x_1 \\ A_{12} = 9000\ \text{J} \cdot \text{mol}^{-1} \\ A_{21} = 7000\ \text{J} \cdot \text{mol}^{-1} \end{cases} \tag{15}$$

The activity coefficients of the two species are derived from the Van Laar g^E model:

$$\gamma_i = \exp\left[\frac{A_{ij}}{RT}\left(\frac{A_{ji}x_j}{A_{ij}x_i + A_{ji}x_j}\right)^2\right], \quad \text{with} \begin{cases} i \neq j \text{ and } (i,j) \in \{1\ ;\ 2\}^2 \\ R = 8.314472\ \text{J} \cdot \text{mol}^{-1} \cdot \text{K}^{-1} \end{cases} \tag{16}$$

The algorithm proposed for the LLE calculation at a fixed temperature using the $\gamma - \varphi$ approach is as follows:

1. Provide initial estimates for the unknowns, for instance: ${x_1'}^{(0)} = 0.01$ and ${x_1''}^{(0)} = 0.99$. Set the iteration counter to: $k = 0$.
2. Calculate $\begin{cases} {\gamma_1'}^{(k)} = \gamma_1({x_1'}^{(k)}) \\ {\gamma_1''}^{(k)} = \gamma_1({x_1''}^{(k)}) \\ {\gamma_2'}^{(k)} = \gamma_2({x_1'}^{(k)}) \\ {\gamma_2''}^{(k)} = \gamma_2({x_1''}^{(k)}) \end{cases}$ from Eq. (16).

3. Define $\delta = [|x'_1\gamma'_1 - x''_1\gamma''_1| + |(1-x'_1)\gamma'_2 - (1-x''_1)\gamma''_2|]^{(k)}$.

   If $\delta < \epsilon$ (where ϵ is the precision afforded, e.g. $\epsilon = 10^{-6}$), then a solution is reached and the procedure is terminated.

4. Update unknowns x'_1 and x''_1 using Eq. (13) and Table 1 (calculation of a LLE using a $\gamma-\varphi$ approach). The iterative scheme can be written as:

$$\begin{cases} {x'_1}^{(k+1)} &= \left[\dfrac{\gamma''_1\cdot(\gamma''_2-\gamma'_2)}{\gamma'_1\cdot\gamma''_2-\gamma''_1\cdot\gamma'_2}\right]^{(k)} \\ {x''_1}^{(k+1)} &= \left[\dfrac{\gamma'_1\cdot(\gamma''_2-\gamma'_2)}{\gamma'_1\cdot\gamma''_2-\gamma''_1\cdot\gamma'_2}\right]^{(k)} = {x'_1}^{(k+1)}\left(\dfrac{\gamma'_1}{\gamma''_1}\right)^{(k)} \end{cases} \tag{17}$$

5. Set $k = k+1$. Return to step 2.

The iterations for the LLE calculation at $T = 300$ K are detailed in Table 2. The proposed algorithm can be used to construct the entire LLE phase diagram, which exhibits an upper critical solution temperature (UCST). To do so, the algorithm has to be run at intermediate temperatures between $T_{\min} = 300$ K (for instance) and $T_{\max} = $ UCST. The same initial estimates for x'_1 and x''_1 can be used for all the LLE calculations (following the first step of the proposed LLE calculation algorithm). Alternatively, in order to increase the speed of convergence, the initial estimates for a given LLE calculation at temperature T can be made at a temperature close to the temperature under consideration.

For the binary system (1) + (2), the coordinates of the upper liquid-liquid critical point are analytically found to be: UCST $\simeq 482.95$ K and $x_{1,\text{crit}} \simeq 0.4073$. The complete LLE diagram, from low temperatures to the UCST and calculated using the proposed algorithm, is shown in Fig. 1(a).

Speed of convergence of the proposed algorithm:

The proposed algorithm is a zeroth-order method since derivatives of the model do not update the mole fractions within the iterative process (see Eq. (13)). A major drawback of this kind of method is the slow convergence that is observed. This feature is illustrated in Fig. 1(b) showing that for temperatures far from the UCST, several dozens of iterations are needed for convergence. When approaching the UCST, convergence is eventually reached after a very large number of iterations. At the critical temperature, this number becomes nearly infinite.

In addition, despite of very poor initial estimates, the proposed algorithm is observed to be remarkably robust and facilitates accurate determination of the compositions of the two liquid

phases in equilibrium, even at temperatures close to the UCST. Furthermore, the calculation procedure requires quite a reasonable computation time: the Fortran 90 program used to calculate the entire LLE diagram in Fig. 1(a) runs in less than 1/10 s, using an Intel Xeon E5345© CPU. Note however that strongly inadequate initial estimates may lead in some rare cases, to the so-called *trivial solution*, producing fluid phases of identical compositions. When constructing the entire phase diagram, such situations can be easily avoided by performing a series of LLE calculations at increasing temperatures where the initial estimates for a LLE calculation at a certain temperature are given by the compositions x_1' and x_1'' from the LLE calculation at the temperature immediately below the prescribed temperature. These efficient initial estimates reduce the number of iterations required for the convergence (see Fig. 1(b)) and more important, generally prevent the trivial solution from being reached, even in the vicinity of the critical temperature.

3.4 Numerical example 2: calculation of liquid-vapor phase equilibrium using an activity-coefficient model for the liquid phase and the ideal gas equation of state for the vapor phase

As an illustration of this case, we consider the binary system acetone(1) + chloroform(2) which is known to exhibit a negative azeotrope. The NRTL (Non-Random Two-Liquid) activity-coefficient model [5] is used to represent the non-ideality of the liquid phase:

$$\frac{g^E(x_1)}{RT} = x_1 x_2 \left[\frac{\tau_{21} \exp(-\alpha\tau_{21})}{x_1 + x_2 \exp(-\alpha\tau_{21})} + \frac{\tau_{12} \exp(-\alpha\tau_{12})}{x_2 + x_1 \exp(-\alpha\tau_{12})} \right], \qquad \text{with} \begin{cases} x_2 = 1 - x_1 \\ \tau_{12} = b_{12}/T \\ \tau_{21} = b_{21}/T \\ b_{12} = 209.38 \text{ K} \\ b_{21} = -431.47 \text{ K} \\ \alpha = 0.1831 \end{cases} \tag{18}$$

The activity coefficients of the two species in the liquid mixture are then given by:

$$\gamma_i = \exp\left[x_j^2 \left[\frac{\tau_{ji} \exp(-2\alpha\tau_{ji})}{\left[x_i + x_j \exp(-\alpha\tau_{ji})\right]^2} + \frac{\tau_{ij} \exp(-\alpha\tau_{ij})}{\left[x_j + x_i \exp(-\alpha\tau_{ij})\right]^2} \right] \right], \quad \text{with} \begin{cases} i \neq j \\ (i,j) \in \{1\ ;\ 2\}^2 \end{cases} \tag{19}$$

The vapor pressures of the pure compounds are given by:

$$\begin{cases} \log\left[P_1^{\text{sat}}(t)/\text{bar}\right] &= 4.2184 - 1197.01/[(t/^\circ\text{C}) + 228.06] \\ \log\left[P_2^{\text{sat}}(t)/\text{bar}\right] &= 3.9629 - 1106.90/[(t/^\circ\text{C}) + 218.55] \end{cases} \tag{20}$$

The pressure of the system is set to $P = 1$ atm. From section 3.1, the proposed algorithm can be written as follows:

1. Provide initial estimates for the unknowns x_1 and y_1. Set the iteration counter to: $k = 0$.
2. Calculate $P_1^{\text{sat}}(T)$ and $P_2^{\text{sat}}(T)$ using Eq. (20).
3. Calculate $\begin{cases} \gamma_1^{(k)} = \gamma_1(x_1^{(k)}) \\ \gamma_2^{(k)} = \gamma_2(x_1^{(k)}) \end{cases}$ from Eq. (19). Calculate the coefficients $C_1^{(k)}$ and $C_2^{(k)}$ using Eq. (4), the pure component liquid molar volume correlations, the pure component vapor pressures correlations and an appropriate EoS for the gas phase.

4. Define $\delta = \left[|Py_1C_1/P_1^{\text{sat}} - x_1\gamma_1| + |P(1-y_1)C_2/P_2^{\text{sat}} - (1-x_1)\gamma_2|\right]^{(k)}$.
   If $\delta < \epsilon$ (where ϵ, is the precision afforded, e.g., $\epsilon = 10^{-6}$), then a solution is reached and the procedure is terminated.

5. Update the unknowns x_1 and y_1:

$$\left\{ \begin{array}{rcl} x_1^{(k+1)} & = & \left[\dfrac{C_1\ (PC_2 - P_2^{\text{sat}}\gamma_2)}{P_1^{\text{sat}}\gamma_1 C_2 - P_2^{\text{sat}}\gamma_2 C_1}\right]^{(k)} \\ y_1^{(k+1)} & = & x_1^{(k+1)} \times \left[P_1^{\text{sat}}\gamma_1/(PC_1)\right]^{(k)} \end{array} \right. \tag{21}$$

6. Set $k = k + 1$. Return to step 3.

At low pressures, the coefficients C_i defined in Eq. (4) are generally assumed to be equal to 1 (the Poynting factor correction is assumed to be equal to 1 and the ideal-gas EoS is used to model the gas-phase behavior). The iterative scheme then reduces to:

$$\left\{ \begin{array}{rcl} x_1^{(k+1)} & = & \left[\dfrac{P - P_2^{\text{sat}}\gamma_2}{P_1^{\text{sat}}\gamma_1 - P_2^{\text{sat}}\gamma_2}\right]^{(k)} \\ y_1^{(k+1)} & = & x_1^{(k+1)} \times \left[P_1^{\text{sat}}\gamma_1/P\right]^{(k)} \end{array} \right. \tag{22}$$

It appears that the two equations in the system given by Eq. (22) can be solved separately and successively (i.e. the two equations can be decoupled). The upper equation only involves the unknown x_1 whereas the lower equation directly yields y_1 as a function of x_1. As a result, the initial estimate for y_1 does not affect the iterative scheme.

Such a situation, which is a particular case of the general solution procedure previously presented, arises because the VLE calculation in binary systems at a specified T and P using the $\gamma - \varphi$ approach at low pressures, reduces to the resolution of a unique equation ($P - P_1^{\text{sat}}x_1\gamma_1 - P_2^{\text{sat}}(1-x_1)\gamma_2 = 0$) with respect to a single unknown (x_1). The iterative scheme takes the form of a classical 1-dimensional direct-substitution method.

This algorithm was applied at $t = 64$ °C ($T = 337.15$ K). At this temperature and atmospheric pressure, the azeotropic system acetone(1) + chloroform(2) exhibits two distinct VLE. The solution that the proposed algorithm converges to, depends on the chosen initial estimate for the unknown x_1. As an illustration, Table 3 shows the results respectively obtained using $x_1^{(0)} = 0.01$ and $x_1^{(0)} = 0.99$.

To plot the complete isobaric phase diagram presented in Fig. 2(a), it was thus necessary to proceed in two steps: the portion of the phase diagram located on the left hand side (*lhs*)

of the negative azeotrope was obtained by performing a succession of VLE calculations at increasing temperatures, using the initial estimate $x_1^{(0)} = 0.01$ systematically. The portion of the phase diagram located on the right hand side (*rhs*) was obtained using a similar procedure with $x_1^{(0)} = 0.99$. Also note that an accurate determination of the azeotrope requires that the temperature step Δt be efficiently managed when calculating each part of the phase diagram. As an example, the temperature can be increased using a constant temperature step (e.g. $\Delta t = 0.1$ K), until a trivial solution (i.e. $x_1 = y_1$) is reached (meaning that the current temperature is above the azeotropic temperature). The temperature is thus returned to its previous value and then increased by using a smaller temperature step (e.g. $\Delta t = \Delta t/10$). The procedure is repeated until $\Delta t < \Delta t_{\min}$ (e.g. $\Delta t_{\min} = 10^{-4}$ K).

It is interesting to note that the proposed algorithm can also be easily used to calculate VLE when the mole fractions of the compounds in the two phases are greater than 1 or less than zero, although this is not relevant for engineering calculations. This feature shows that the algorithm does not necessarily diverge at the specified temperature and pressure when no physically meaningful VLE exists. Fig. 2(b) shows that convergence is reached after quite a reasonable number of iterations for each VLE calculation. When the phase diagram does not exhibit criticality, a few dozens of iterations are generally required. Note that this number reaches a minimum at the pure-component VLE point.

On the choice of initial estimates for x_1:

Since the VLE calculation reduces to solve one equation with respect to x_1 when using the $\gamma - \varphi$ approach with $C_i = 1$, an initial value is not needed for the unknown y_1 and an initial estimate may be easily chosen for x_1, as explained below.

First of all, note that it is simple to choose the initial estimate in most of the cases where the liquid-vapor phase diagram does not exhibit azeotropy or a three-phase line (or any combination of both). In such cases and if a VLE exists at the specified temperature and pressure, then any value of $x_1 \in]0\ ;\ 1[$ leads to a correct solution (divergence problems are quite scarce).

As previously mentioned, phase diagrams exhibiting azeotropy are trickier to deal with since two VLE may exist at a fixed temperature and pressure. The case of the binary system acetone(1) + chloroform(2) at atmospheric pressure is reconsidered as an illustration. Three different situations may occur:

- the calculation converges to a solution such that $x_1 > y_1$ which is located in the left hand

side (*lhs*) of the phase diagram shown in Fig. 2(a)

- the calculation converges to a solution such that $x_1 < y_1$ which is located in the right hand side (*rhs*) of the phase diagram shown in Fig. 2(a)

- or the calculation diverges.

The three domains associated with each of these three situations are shown in Fig. 3. The domain of divergence is large at low temperatures, narrows with increasing temperature and reduces to a single point at the azeotropic temperature. This figure also illustrates why the initial estimates $x_1^{(0)} = 0.01$ and $x_1^{(0)} = 0.99$ can be used to construct the phase diagram at all temperatures without difficulty. Since the domain of divergence generally occurs in the middle of the composition range, it is advisable to systematically choose initial x_1 estimates close to zero and one.

More details on the fixed point method and convergence-related issues can be found in Appendix A.

3.5 Numerical example 3: calculation of a fluid-fluid phase equilibrium using an equation of state

In this section, the Peng-Robinson EoS [6] is used to model the liquid-vapor phase behavior of the binary system carbon dioxide(1) + n-hexane(2) at $T = 393.15$ K and $P = 40$ bar. The Peng-Robinson EoS is given by:

$$P_{\text{EoS}}(T, v, z_i) = \frac{RT}{v - b_m} - \frac{a_m}{v(v + b_m) + b_m(v - b_m)} \tag{23}$$

where P_{EoS} is the pressure of the mixture calculated from the EoS, v is the molar volume of the fluid; z_i is the mole fraction of component i in the fluid phase under consideration ($z_i = x_i$ for a liquid phase and $z_i = y_i$ for a gas phase); and a_m and b_m are the two EoS parameters for the mixture, which follow the classical mixing rules given below:

$$a_m = \sum_{i=1}^{2}\sum_{j=1}^{2} z_i z_j \sqrt{a_i a_j}\,(1 - k_{ij}) \qquad \text{and} \qquad b_m = \sum_{i=1}^{2} z_i b_i \tag{24}$$

Expressions for the pure-component quantities a_i and b_i are provided in Table 4. The critical temperatures, critical pressures and acentric factors of the pure components that are needed to evaluate the coefficients a_i and b_i, are given in Table 5. The binary interaction parameters

are estimated using the PPR78 group-contribution method [7, 8]: $k_{12} = k_{21} = 0.1178$ and $k_{11} = k_{22} = 0$. As explained in section 2.2, a pressure-explicit EoS for mixtures that can represent both a liquid and a vapor phase, as opposed to a volume-explicit EoS, uses the temperature T, the molar volume v and the composition as variables. Consequently, the fluid-fluid equilibrium problem at a fixed T and P involves solving four equations (see Eq. (7)) with respect to four unknowns: the molar volumes and compositions of the two phases in equilibrium. In the Peng-Robinson EoS, the fugacity coefficient of a given compound i in a phase characterized by the temperature T, the molar volume v, the mole fractions z_i of the compounds and the pressure $P = P_{\text{EoS}}(T, v, z_i)$, is given by:

$$\begin{cases} \ln \hat{\varphi}_i = \dfrac{b_i}{b_m}\left(\dfrac{Pv}{RT} - 1\right) - \ln\left[\dfrac{P(v-b_m)}{R \cdot T}\right] - \dfrac{a_m}{2\sqrt{2}\,RTb_m}\left(\delta_i - \dfrac{b_i}{b_m}\right) \cdot \ln\left[\dfrac{v + b_m(1+\sqrt{2})}{v + b_m(1-\sqrt{2})}\right] \\ \text{with: } \delta_i = 2\dfrac{\sqrt{a_i}}{a_m}\displaystyle\sum_{j=1}^{n_c} z_j\sqrt{a_j}\,(1-k_{ij}) \end{cases} \tag{25}$$

The following algorithm is proposed for solving a liquid-vapor equilibrium at a specified T and P, modeled with an EoS:

1. Provide initial estimates for the unknown mole fractions, for instance: $[x_1]^{(0)} = 0.01$ and $[y_1]^{(0)} = 0.99$. Set the iteration counter to: $k = 0$.

2. Calculate the molar volumes of the liquid and gas phases at the current iteration k (denoted by $v_L^{(k)}$ and $v_G^{(k)}$) by solving the EoS at a fixed T, P and composition:

$$\begin{cases} v_L^{(k)} \text{ is the solution of the equation:} & P = P_{\text{EoS}}(T, v_L^{(k)}, x_1^{(k)}) \\ v_G^{(k)} \text{ is the solution of the equation:} & P = P_{\text{EoS}}(T, v_G^{(k)}, y_1^{(k)}) \end{cases} \tag{26}$$

   Note that the resolution of an EoS is a recurring thermodynamic issue, addressed many times [9, 10]. For a cubic EoS, a simple Cardano-type method can be used.

   In addition, the solution of the EoS may produce either one or three roots. When the EoS has three roots, the liquid root has the smallest molar volume whereas the vapor root has the highest molar volume.

3. Calculate the fugacity coefficients of all components in all phases:

$$\forall i \in \{1\ ;\ 2\} \quad \begin{cases} \hat{\varphi}_{i,L}^{(k)} = \hat{\varphi}_i(T, v_L^{(k)}, x_1^{(k)}) \\ \hat{\varphi}_{i,G}^{(k)} = \hat{\varphi}_i(T, v_G^{(k)}, y_1^{(k)}) \end{cases} \tag{27}$$

4. Define $\delta = [|x_1\hat{\varphi}_{1,L} - y_1\hat{\varphi}_{1,G}| + |(1-x_1)\hat{\varphi}_{2,L} - (1-y_1)\hat{\varphi}_{2,G}|]^{(k)}$.

   If $\delta < \epsilon$ (where ϵ is the afforded precision, e.g. $\epsilon = 10^{-6}$), then a solution is reached and the procedure is terminated.

5. Update the unknowns x_1 and y_1: from Eq. (13) and Table 1 (calculation of a VLE using a $\varphi - \varphi$ approach), the iterative scheme may be written as:

$$\left\{ \begin{array}{rcl} x_1^{(k+1)} & = & \left[\dfrac{\hat{\varphi}_{1,G} \cdot (\hat{\varphi}_{2,G} - \hat{\varphi}_{2,L})}{\hat{\varphi}_{1,L} \cdot \hat{\varphi}_{2,G} - \hat{\varphi}_{1,G} \cdot \hat{\varphi}_{2,L}} \right]^{(k)} \\ y_1^{(k+1)} & = & \left[\dfrac{\hat{\varphi}_{1,L} \cdot (\hat{\varphi}_{2,G} - \hat{\varphi}_{2,L})}{\hat{\varphi}_{1,L} \cdot \hat{\varphi}_{2,G} - \hat{\varphi}_{1,G} \cdot \hat{\varphi}_{2,L}} \right]^{(k)} = x_1^{(k+1)} \left(\dfrac{\hat{\varphi}_{1,L}}{\hat{\varphi}_{1,G}} \right)^{(k)} \end{array} \right. \tag{28}$$

6. Set $k = k + 1$. Return to step 2.

Details of the calculation of the liquid-vapor equilibrium for the binary system CO_2 + n-hexane at 393.15 K and 40 bar are given in Table 6. Repeating this procedure at different pressures while holding the temperature constant allows generating the complete fluid phase diagram at 393.15 K, as shown in Fig. 4(a). Note that this diagram culminates in a liquid-vapor critical point. More precisely, the phase diagram is constructed simply by solving the phase equilibrium equations at gradually increasing pressures. The only difficulty is found in the vicinity of the critical point: at $P > P_c$ (where P_c denotes the critical pressure of the mixture), no phase equilibrium exists and the algorithm finds a trivial solution; at $P < P_c$, the solution of the phase-equilibrium problem is easily found regardless of the initial estimates for the mole fractions x_1 and y_1. However, the nearer the pressure is to the critical pressure, the closer are the compositions of both the equilibrium phases. Therefore, the following procedure is recommended for obtaining a phase diagram that accurately captures the critical region:

1. Specify T and set P to P_{init} (e.g. $P_{\text{init}} = 1$ bar).

2. Specify the pressure step, e.g. $\Delta P = 1$ bar.

3. Set the initial values: $k = 0$, $x_1^{(k)} = 0.01$ and $y_1^{(k)} = 0.99$.

4. Solve the VLE problem at the current values of T and P using the algorithm presented above. A tolerance of $\epsilon = 10^{-10}$ is recommended.

5. **If** $|x_1 - y_1| > \epsilon'$ (e.g. $\epsilon' = 10^{-5}$), **then** a non-trivial solution is found which is acceptable.

   A new value of P is specified such that $P = P + \Delta P$; return to step 3.

Else, a trivial solution is found which is rejected: the current pressure is thus above the critical pressure. The pressure is then decreased to the pressure of the last successful VLE calculation: $P = P - \Delta P$. The pressure is then increased again with a smaller step: $\Delta P = \Delta P/10$ and $P = P + \Delta P$.

If $\Delta P < \Delta P_{\mathbf{min}}$ (e.g. $\Delta P_{\min} = 10^{-4}$ bar), **then** the procedure is terminated;

Else, return to step 3.

Note that the values chosen for ϵ, ϵ' and $\Delta P_{\min}$ are all interrelated and must be adjusted depending on the case study under consideration. The proposed values are the ones that were used to calculate the phase diagram shown in Fig. 4(a).

Fig. 4(b) shows that few iterations are needed for calculations far from the critical point whereas the number of iterations approaches infinity in the vicinity of the critical point. As previously noted, the proposed algorithm easily calculates fictitious equilibria characterized by mole fractions greater than one or less than zero in domains of temperatures and pressures when the binary system is in a single phase. In addition, the minimum number of iterations is found at the pure-component VLE point.
Mathematical details on the convergence of two-dimensional direct-substitution methods can be found in Appendix B.

4 Derivation of a new algorithm for phase-equilibrium calculation in ternary systems at a fixed temperature and pressure

4.1 General solution procedure

Following Eq. (8), the general form of the phase equilibrium relations in a ternary system may be written as follows:

$$x'_i F'_i = x''_i F''_i, \quad \forall i \in [\![1\ ;\ 3]\!] \tag{29}$$

The form of the F_i functions depends on the selected approach ($\gamma-\varphi$ or $\varphi-\varphi$) and sometimes (as for the $\gamma-\varphi$ approach) on the nature of the phase equilibrium (VLE or LLE) involved, as shown in Table 1. At a fixed temperature and pressure, four variables are associated with the two-phase equilibrium problem: x'_1, x'_2, x''_1 and x''_2; note that the two remaining composition variables,

x_3' and x_3'', are not considered since they can be directly obtained from the two summation relationships: $x_3' = 1 - x_1' - x_2'$ and $x_3'' = 1 - x_1'' - x_2''$. In summary, at fixed T and P, there are three phase-equilibrium equations and four variables, leaving one degree of freedom. One variable among the four must be specified to solve the problem, with the three remaining variables making up the set of unknowns. The phase equilibrium problem in ternary systems at a fixed temperature and pressure then involves solving the following set of four equations with respect to the four aforementioned unknowns:

$$\begin{cases} x_1' F_1' & = & x_1'' F_1'' \\ x_2' F_2' & = & x_2'' F_2'' \\ (1 - x_1' - x_2') F_3' & = & (1 - x_1'' - x_2'') F_3'' \\ \multicolumn{3}{c}{\text{Specification equation}} \end{cases} \tag{30}$$

The specification equation may apply to any of the six composition variables, e.g. $x_1' = s$ (where s denotes the value of the specified variable), or $x_2'' = s$, or $x_3' = s \Leftrightarrow 1 - x_1' - x_2' = s$.

As in binary systems, the system of equations (30) can be equivalently expressed by matrix notation in the following form:

$$\mathbf{A}\,\mathbf{X} = \mathbf{B} \tag{31}$$

where $\mathbf{X}$ represents the vector of unknowns:

$$\mathbf{X} = \begin{pmatrix} x_1' \\ x_2' \\ x_1'' \\ x_2'' \end{pmatrix} \tag{32}$$

The last line of the matrix $\mathbf{A}$ and the vector $\mathbf{B}$ depends on the choice of the specification equation. For instance, choosing $x_2' = s$ as a specification equation, one obtains:

$$\mathbf{A} = \begin{pmatrix} F_1' & 0 & -F_1'' & 0 \\ 0 & F_2' & 0 & -F_2'' \\ -F_3' & -F_3' & F_3'' & F_3'' \\ 0 & 1 & 0 & 0 \end{pmatrix} \quad \text{and} \quad \mathbf{B} = \begin{pmatrix} 0 \\ 0 \\ F_3'' - F_3' \\ s \end{pmatrix} \tag{33}$$

Otherwise, choosing $x_3'' = s \Leftrightarrow x_1'' + x_2'' = 1 - s$ as a specification equation produces:

$$\mathbf{A} = \begin{pmatrix} F_1' & 0 & -F_1'' & 0 \\ 0 & F_2' & 0 & -F_2'' \\ -F_3' & -F_3' & F_3'' & F_3'' \\ 0 & 0 & 1 & 1 \end{pmatrix} \quad \text{and} \quad \mathbf{B} = \begin{pmatrix} 0 \\ 0 \\ F_3'' - F_3' \\ 1 - s \end{pmatrix} \tag{34}$$

An iterative scheme can be deduced from Eq. (31) similar to that developed for binary systems, by solving the phase equilibrium problem for ternary systems at a fixed T, P for a given value of one composition variable. The mole fraction values at iteration $(k+1)$ are thus deduced from the mole fraction values at iteration k as follows:

$$\underbrace{\begin{pmatrix} x_1' \\ x_2' \\ x_1'' \\ x_2'' \end{pmatrix}^{(k+1)}}_{\mathbf{X}^{(k+1)}} = \left[\mathbf{A}(\mathbf{X}^{(k)})\right]^{-1} \mathbf{B}(\mathbf{X}^{(k)}) \tag{35}$$

4.2 Calculation of isothermal isobaric ternary phase diagrams using a $\varphi - \varphi$ approach

First, the nitrogen(1) + methane(2) + ethane(3) system at $T = 200$ K and $P = 80$ bar is studied to illustrate the capability of the phase equilibrium calculation algorithm. The properties of the corresponding pure components are given in Table 5. The Peng-Robinson EoS is used again to model the thermodynamic behavior of the fluid mixture. The binary interaction coefficients are all set to zero in this case study: $k_{ij} = 0,\ \forall (i,j) \in [\![1\ ;\ 3]\!]^2$. Among the three binary systems that can be defined by this ternary system, only the $N_2(1)$ + ethane(3) mixture gives rise to a two-fluid-phase equilibrium under the selected T and P conditions. Consequently, in the neighborhood of the two-phase equilibrium of the binary system (1) + (3), the ternary system certainly exhibits a two-phase equilibrium region. This motivates choosing either x_2' or x_2'' as a specified composition variable and using a very small initial value (e.g. $x_2' = 10^{-4}$). Note that the phase equilibrium of the binary system (1) + (3) can be calculated by specifying $x_2' = 0$. The strategy for constructing the entire isothermal and isobaric ternary phase diagram is now explained in detail.

1. Specify the working temperature and pressure.

2. Set the value of the specified composition variable: $s = 10^{-4}$.

3. Set the initial estimates: $x'_1 = 0.01$, $x'_2 = s$ and $x'_3 = 1 - x'_1 - x'_2$.
   $x''_1 = 0.99$, $x''_2 = 0$ (and thus $x''_3 = 1 - x''_1$).
   Set the iteration counter to: $k = 0$.

4. Determine the molar volumes of the phases ($v_L^{(k)}$ and $v_G^{(k)}$) at the current iteration k and the specified T, P and estimated compositions of the phases by solving the Peng-Robinson EoS:
$$\begin{cases} v_L^{(k)} \text{ is the solution of the equation:} & P = P_{\text{EoS}}(T, v_L^{(k)}, x_i'^{(k)}) \\ v_G^{(k)} \text{ is the solution of the equation:} & P = P_{\text{EoS}}(T, v_G^{(k)}, x_i''^{(k)}) \end{cases} \tag{36}$$

5. Calculate the fugacity coefficients of all components in all phases:
$$\forall i \in [\![1\ ;\ 3]\!] \quad \begin{cases} \hat{\varphi}_i'^{\,(k)} = \hat{\varphi}_i(T, v_L^{(k)}, x_i'^{(k)}) \\ \hat{\varphi}_i''^{\,(k)} = \hat{\varphi}_i(T, v_G^{(k)}, x_i''^{(k)}) \end{cases} \tag{37}$$

6. Define $\delta = \sum_{i=1}^{3} \left| x'_i \hat{\varphi}'_i - x''_i \hat{\varphi}''_i \right|^{(k)}$. If $\delta < \epsilon$ (where ϵ is the precision afforded, e.g., $\epsilon = 10^{-10}$), then a solution is reached; proceed to step 9.

7. Calculate the matrix $\mathbf{A}$ and the vector $\mathbf{B}$ at the current iteration k:
$$\mathbf{A}^{(k)} = \begin{pmatrix} \hat{\varphi}'_1 & 0 & -\hat{\varphi}''_1 & 0 \\ 0 & \hat{\varphi}'_2 & 0 & -\hat{\varphi}''_2 \\ -\hat{\varphi}'_3 & -\hat{\varphi}'_3 & \hat{\varphi}''_3 & \hat{\varphi}''_3 \\ 0 & 1 & 0 & 0 \end{pmatrix}^{(k)} \quad \text{and} \quad \mathbf{B}^{(k)} = \begin{pmatrix} 0 \\ 0 \\ \hat{\varphi}''_3 - \hat{\varphi}'_3 \\ s \end{pmatrix}^{(k)} \tag{38}$$

8. Update the unknowns x'_i and x''_i using Eq. (35). Note that the 4×4 matrix $\mathbf{A}$ can be inverted using the so-called *LU decomposition method*, for instance. Proceed to step 4.

9. Increase the value for the specified variable: $s = s + \Delta s$ (e.g., $\Delta s = 10^{-3}$) and return to step 4.
   If $x'_i > 1$ or $x'_i < 0$ or $x''_i > 1$ or $x''_i < 0$ ($\forall i \in [\![1\ ;\ 3]\!]$), then the phase diagram is complete and the procedure is terminated.
   If a critical point arises in the phase diagram (which is the case for the N_2 + methane + ethane system at 200 K and 80 bar), then trivial solutions may be obtained. These trivial solutions are dealt with exactly as for the binary systems (see sections 3.3 and 3.5).

The left hand side of Fig. 5 shows the fluid-phase behavior of the aforementioned system in a triangular diagram calculated using the algorithm above. The shape of a liquid-liquid phase diagram is observed, culminating in a liquid-liquid critical point. The right hand side of Fig. 5 shows the number of iterations required for each phase-equilibrium calculation, plotted as a function of the specified variable x_2'. This number is once more observed to approach infinity in the vicinity of the critical point.

As another illustration, Fig. 6 shows the phase diagram of the ternary system $CO_2(1)$ + propane(2) + ethane(3) at 230 K and 11 bar calculated using the Peng-Robinson EoS. Binary interaction coefficients were considered for CO_2 + alkane binary mixtures: $k_{CO_2/\text{alkane}} = 0.15$. For this system and because of the banana shape of the two-phase region, the most convenient variables to specify are either x_3 or y_3. The variable y_3 was chosen for the present case and fixed at $s = 0.237$ for the first ternary phase equilibrium calculation (note that this value was deduced from the calculation of the two-phase equilibrium of the binary system (1) + (3) at 230 K and 11 bar). The matrix $\mathbf{A}$ is then given by Eq. (34). The 'Iteration number' versus y_3 diagram given in Fig. 6 shows that several dozen iterations are systematically needed for convergence.

5 Conclusion

Most zeroth-order algorithms used in two-phase equilibrium calculations (e.g., the bubble pressure algorithm, the dew temperature algorithm ...) are generally time-consuming since a main loop is combined with a nested loop to iterate on the two sets of variables associated with each of the two equilibrium phases. In the present work, because of re-casting the problem in matrix notation, only one loop is used to iterate simultaneously on both sets of variables.

Another advantage of the proposed algorithm is that it may be applied to both binary and ternary systems, and more interestingly, can treat any kind of phase equilibrium (VLE, LLE ...) regardless of the chosen approach ($\varphi - \varphi$ or $\gamma - \varphi$) whereas other algorithms generally only apply to one phase-equilibrium type and one given approach. As all the formalisms and related solution procedures in the phase-equilibrium calculation have been unified, the proposed algorithm is claimed to be universal.

A third advantage has been pointed out in the body of the paper: the choice of the initial estimates for the unknowns has little impact on convergence even when calculating phase equilibria

near azeotropic points.

It could be remarked that more powerful and complex algorithms can perform the kind of calculations presented in this paper but the proposed tool does not conflict with these more complex algorithms by any means. The current tool is appropriate for people working on thermodynamic issues (model development, simulation, process design ...) who do not use commercial softwares. We should also mention that the proposed algorithm can be quite useful where commercial software fails in calculating phase diagrams exhibiting singularities (criticality, azeotropy and so on).

After solving the two-phase equilibrium problem with the proposed algorithm, it is advisable to test the stability of the resulting phases to check whether the obtained solution is the most stable one under the specified conditions. In order to avoid undesirable results, the proposed algorithm should be coupled with an algorithm based on the tangent plane distance criterion [11] to discriminate between stable and non-stable phases.

A Information on the direct-substitution method applied to VLE calculations under low pressure using a $\gamma - \varphi$ approach

A.1 Description of the q function

Under the conditions given above and as explained in section 3.4, the VLE problem at a fixed T and P results in a direct-substitution problem (see Eq. (22)):

$$q(x_1) = x_1 \qquad \text{with: } q(x_1) = \frac{P - P_2^{\text{sat}}\gamma_2}{P_1^{\text{sat}}\gamma_1 - P_2^{\text{sat}}\gamma_2} \tag{39}$$

For non-azeotropic systems at a T and P such that a VLE exists, the q function exhibits two fixed points and a vertical asymptote (associated with a null denominator: $P_1^{\text{sat}}\gamma_1 - P_2^{\text{sat}}\gamma_2 = 0$). This behavior is illustrated in Fig. 7. Only the first fixed point is associated with the actual VLE (where $0 \leq x_1 \leq 1$) whereas the second fixed point can be found at $x^* > 1$. It can be proved using standard mathematical tools (alternating and monotone sequence theorems) that any initial estimate $x_1 \in [0\ ;\ 1]$ results in convergence to the first fixed point (and more generally, that convergence is guaranteed for any initial estimate satisfying $0 < x_1 < x^*$). The iterative process diverges for an initial estimate such that $x_1 > x^*$. Note that for binary systems exhibiting ideal liquid behavior ($\gamma_i = 1$), the q function no longer depends on x_1:

$$q(x_1) = \frac{P - P_2^{\text{sat}}}{P_1^{\text{sat}} - P_2^{\text{sat}}} \tag{40}$$

and the q function is a straight horizontal line, indicating the existence of a single fixed point. In this case - and for all systems exhibiting small departures from ideality - the iterative process is strictly always convergent.

The shape of the q function is a little different for azeotropic systems, as illustrated in Fig. 8. Indeed, at a specified pressure and temperature lower than the azeotropic temperature ($t_{\text{azeotrope}}$), such that two VLE are found, the q function exhibits three fixed points, the first two being associated with the actual VLE. As previously mentioned, an additional fixed point exists at a mole fraction x^* greater than one. Only the third fixed point persists at a temperature above the azeotropic temperature.

A.2 On the convergence and divergence of iterative processes

Let us recall that essentially two factors impact the convergence of a fixed-point algorithm for solving an equation of the type $q(x_1) = x_1$:

- the value of the derivative $|q'(x_{\text{fp}})|$, where x_{fp} is the coordinate of the fixed point. Then,
  - if $|q'(x_{\text{fp}})| < 1$, the fixed-point method will converge to the fixed point with coordinates $(x_{\text{fp}}, x_{\text{fp}})$ assuming an appropriate initial estimate for x_1. The fixed point is then called *attractive*.
  - if $|q'(x_{\text{fp}})| > 1$, the fixed-point method will diverge. The corresponding fixed point is called *repulsive*.
  - if $|q'(x_{\text{fp}})| = 1$, the fixed-point iterative process will be either divergent or convergent (more detailed analysis is needed to draw a conclusion).

  Fig. 9 illustrates this instance. The first two fixed points are associated with a derivative $|q'(x_{\text{fp}})| < 1$ and are thus attractive. The third fixed point is associated with a derivative $q'(x_{\text{fp}}) > 1$ and is thus repulsive.

- the quality of the initial estimate.

  For $|q'(x_{\text{fp}})| < 1$, the fixed-point method converges in the vicinity of the fixed point. It thus becomes possible to define a *basin of attraction* that contains all the initial estimate values that lead to a converging iterative process.

  The sensitivity of the fixed-point method with respect to the initial estimates was discussed in section 3.4 and illustrated in Fig. 3 where the basins of attraction (i.e. the domains of convergence) are shown. At a fixed T and P such that two VLE exist, one observes that a domain of divergence (denoted by $[x_{\text{lim},1}, x_{\text{lim},2}]$) in the composition range [0 ; 1], systematically exists (i.e., any initial value of x_1 within this domain will cause the fixed-point method to diverge).

  Graphical construction shows that for any $x_1 \in [x_{\text{lim},1}, x_{\text{lim},2}]$, the fixed-point method almost immediately produces x_1 values greater than x^*, the coordinate of the repulsive fixed point, thus explaining the diverging process. By using the borderline values $x_{\text{lim},1}$ and $x_{\text{lim},2}$ as initial estimates, the fixed-point method converges exactly to the repulsive fixed point (x^*, x^*), as shown in Fig. 10.

B On the convergence of the direct-substitution method as applied to two-dimensional problems

This section shows how the conclusions presented in Appendix A (which dealt with the convergence of the one-dimensional direct-substitution method) can be generalized to two-dimensional problems.

As shown in the body of the paper, the two-phase equilibrium problem for binary systems at fixed temperature and pressure, can be expressed by the following general form:

$$\begin{cases} q_1(\mathbf{X}) &= X_1 \\ q_2(\mathbf{X}) &= X_2 \end{cases} \tag{41}$$

with $X_1 = x_1'$, the mole fraction of component 1 in one phase, and $X_2 = x_1''$ the mole fraction of component 1 in the other phase.

Let us denote a fixed point by $\mathbf{X_{fp}}$ and the Jacobian matrix associated with the $\mathbf{q}$ function by $q_{ij}' = \partial q_i / \partial X_j$. The two eigenvalues of $\mathbf{q}'$ are denoted λ_1 and λ_2 ($\lambda_i \in \mathbb{C}$); they are not necessarily distinct.

The convergence of the two-dimensional direct-substitution process obeys the following rules:

- if $\mathbf{q}'(\mathbf{X_{fp}})$ has at least one eigenvalue satisfying $|\lambda_i| > 1$, initial estimates can be found that are arbitrarily close to the fixed point such that the method is divergent.
- if all the eigenvalues of $\mathbf{q}'(\mathbf{X_{fp}})$ satisfy $|\lambda_i| < 1$, an open set containing $\mathbf{X_{fp}}$ exists such that any initial estimate chosen within this open set makes the method convergent.
- if there is one eigenvalue such that $|\lambda_i| = 1$ (and the other eigenvalue satisfies $|\lambda_i| \leq 1$) then the iterative process will be either divergent or convergent (and more detailed analysis is needed to draw a conclusion).

Remark: the convergence of the direct-substitution method can be accelerated by using Aitken's delta-squared process, for instance.

References

[1] S. I. Sandler. *Chemical, biochemical, and engineering thermodynamics, fourth edition*. John Wiley & Sons, 2006.

[2] M. L. Michelsen. Saturation point calculations. *Fluid Phase Equilibria*, 23(2-3):181–192, 1985.

[3] J. M. Smith and H.C. Van Ness. *Introduction to chemical engineering thermodynamics, third edition*. Mc Graw-Hill, 1975.

[4] A. Lucia, X. Guo, P. J. Richey, and R. Derebail. Simple process equations, fixed-point methods, and chaos. *AIChE Journal*, 36(5):641–654, 1990.

[5] H. Renon and J. M. Prausnitz. Local compositions in thermodynamic excess functions for liquid mixtures. *AIChE Journal*, 14(1):135–144, 1968.

[6] D.-Y. Peng and D. B. Robinson. A new two-constant equation of state. *Industrial & Engineering Chemistry Fundamentals*, 15(1):59–64, 1976.

[7] J.-N. Jaubert and F. Mutelet. VLE predictions with the Peng-Robinson equation of state and temperature dependent k_{ij} calculated through a group contribution method. *Fluid Phase Equilibria*, 224(2):285–304, 2004.

[8] J.-N. Jaubert, R. Privat, and F. Mutelet. Predicting the phase equilibria of synthetic petroleum fluids with the PPR78 approach. *AIChE J.*, 56(12):3225–3235, 2010.

[9] U. K. Deiters. Calculation of densities from cubic equations of state. *AIChE Journal*, 48(4):882–886, 2002.

[10] R. Privat, R. Gani, and J.-N. Jaubert. Are safe results obtained when the PC-SAFT equation of state is applied to ordinary pure chemicals? *Fluid Phase Equilib.*, 295(1):76 – 92, 2010.

[11] M. L. Michelsen and J. M. Mollerup. *Thermodynamics Models : Fundamentals and Computational Aspects*. GP-Tryk A/S, Denmark, 2004.

List of Tables

Table 1. Expressions of functions F_1 and F_2 appearing in Eq. (8).

Approach:	$\gamma - \varphi$ approach		$\varphi - \varphi$ approach
Type of phase-equilibrium calculation:	VLE	LLE	Fluid-fluid equilibrium
F_1'	γ_1	γ_1'	$\hat{\varphi}_1'$
F_1''	$P \cdot C_1 / P_1^{\mathrm{sat}}$	γ_1''	$\hat{\varphi}_1''$
F_2'	γ_2	γ_2'	$\hat{\varphi}_2'$
F_2''	$P \cdot C_2 / P_2^{\mathrm{sat}}$	γ_2''	$\hat{\varphi}_2''$

Table 2. Iteration details of the LLE calculation performed in section 3.3.

Iteration	x_1'	x_1''	γ_1'	γ_1''	γ_2'	γ_2''	$\log \delta$
	0.01000	**0.99000**					
1	0.02789	0.93862	28.67378	1.00849	1.00356	12.69554	-0.46
2	0.03248	0.92352	27.54304	1.01330	1.00482	11.90531	-0.99
3	0.03379	0.91845	27.23057	1.01517	1.00521	11.65221	-1.48
4	0.03417	0.91668	27.13949	1.01585	1.00533	11.56517	-1.95
5	0.03429	0.91605	27.11251	1.01610	1.00536	11.53453	-2.43
6	0.03432	0.91583	27.10447	1.01619	1.00537	11.52365	-2.89
7	0.03433	0.91575	27.10207	1.01622	1.00538	11.51977	-3.36
8	0.03434	0.91572	27.10135	1.01623	1.00538	11.51839	-3.82
9	0.03434	0.91571	27.10114	1.01623	1.00538	11.51790	-4.28
10	0.03434	0.91571	27.10107	1.01624	1.00538	11.51772	-4.74
11	0.03434	0.91571	27.10105	1.01624	1.00538	11.51766	-5.19
12	0.03434	0.91571	27.10105	1.01624	1.00538	11.51764	-5.65
13	0.03434	0.91571	27.10105	1.01624	1.00538	11.51763	-6.10

Table 3. Iteration details for the two VLE calculations performed in section 3.4 using two different initial estimates for unknown x_1.

Iteration	x_1	y_1	$\log \delta$
	0.01000		
1	0.20795	0.00636	-0.67
2	0.23475	0.16184	-1.46
3	0.23003	0.18760	-2.20
4	0.23115	0.18298	-2.83
5	0.23090	0.18407	-3.47
6	0.23095	0.18382	-4.11
7	0.23094	0.18388	-4.76
8	0.23094	0.18386	-5.40
9	0.23094	0.18387	-6.04

Iteration	x_1	y_1	$\log \delta$
	0.99000		
1	0.66050	1.28752	-0.14
2	0.60094	0.75855	-0.94
3	0.62039	0.66233	-1.44
4	0.61130	0.69334	-1.77
5	0.61513	0.67879	-2.15
6	0.61343	0.68491	-2.50
7	0.61417	0.68219	-2.86
8	0.61384	0.68337	-3.22
9	0.61398	0.68286	-3.58
10	0.61392	0.68308	-3.94
11	0.61395	0.68298	-4.30
12	0.61394	0.68303	-4.66
13	0.61394	0.68301	-5.02
14	0.61394	0.68301	-5.38
15	0.61394	0.68301	-5.74
16	0.61394	0.68301	-6.10

Table 4. Parametrization of the Peng-Robinson EoS.

Quantity	Expression
Critical compacity η_c	$\frac{1}{3}\left(-1+\sqrt[3]{6\sqrt{2}+8}-\sqrt[3]{6\sqrt{2}-8}\right)$
Universal constant Ω_a	$8(5\eta_c+1)/(49-37\eta_c)$
Universal constant Ω_b	$\eta_c/(\eta_c+1)$
Shape function m_i	$0.37464+1.54226\omega_i-0.26992\omega_i^2$
$a_{c,i}$	$\Omega_a R^2 T_{c,i}^2/P_{c,i}$
b_i	$\Omega_b R T_{c,i}/P_{c,i}$
$\alpha_i(T)$	$\left[1+m_i\left(1-\sqrt{T/T_{c,i}}\right)\right]^2$
$a_i(T)$	$a_{c,i}\,\alpha_i(T)$

Table 5. Physical properties of pure components.

	T_c/K	P_c/MPa	ω
CO_2	304.2	7.383	0.2236
n-hexane	507.6	3.025	0.3013
N_2	126.2	3.400	0.0377
methane	190.6	4.599	0.0120
ethane	305.3	4.872	0.0990
propane	369.8	4.248	0.1520

Table 6. Iteration details of the VLE calculation performed in section 3.5.

Iteration k	x_1	y_1	$v_L/(\mathrm{dm}^3 \cdot \mathrm{mol}^{-1})$	$v_G/(\mathrm{dm}^3 \cdot \mathrm{mol}^{-1})$	$\log \delta$
	0.01000	**0.99000**			
1	0.19632	0.86966	0.14930	0.74349	-0.02
2	0.21851	0.84785	0.13997	0.70000	-0.94
3	0.22219	0.84312	0.13917	0.68982	-1.69
4	0.22285	0.84206	0.13905	0.68751	-2.41
5	0.22296	0.84182	0.13903	0.68699	-3.11
6	0.22298	0.84177	0.13902	0.68687	-3.81
7	0.22299	0.84175	0.13902	0.68685	-4.50
8	0.22299	0.84175	0.13902	0.68684	-5.19
9	0.22299	0.84175	0.13902	0.68684	-5.87
10	0.22299	0.84175	0.13902	0.68684	-6.55

List of Figures

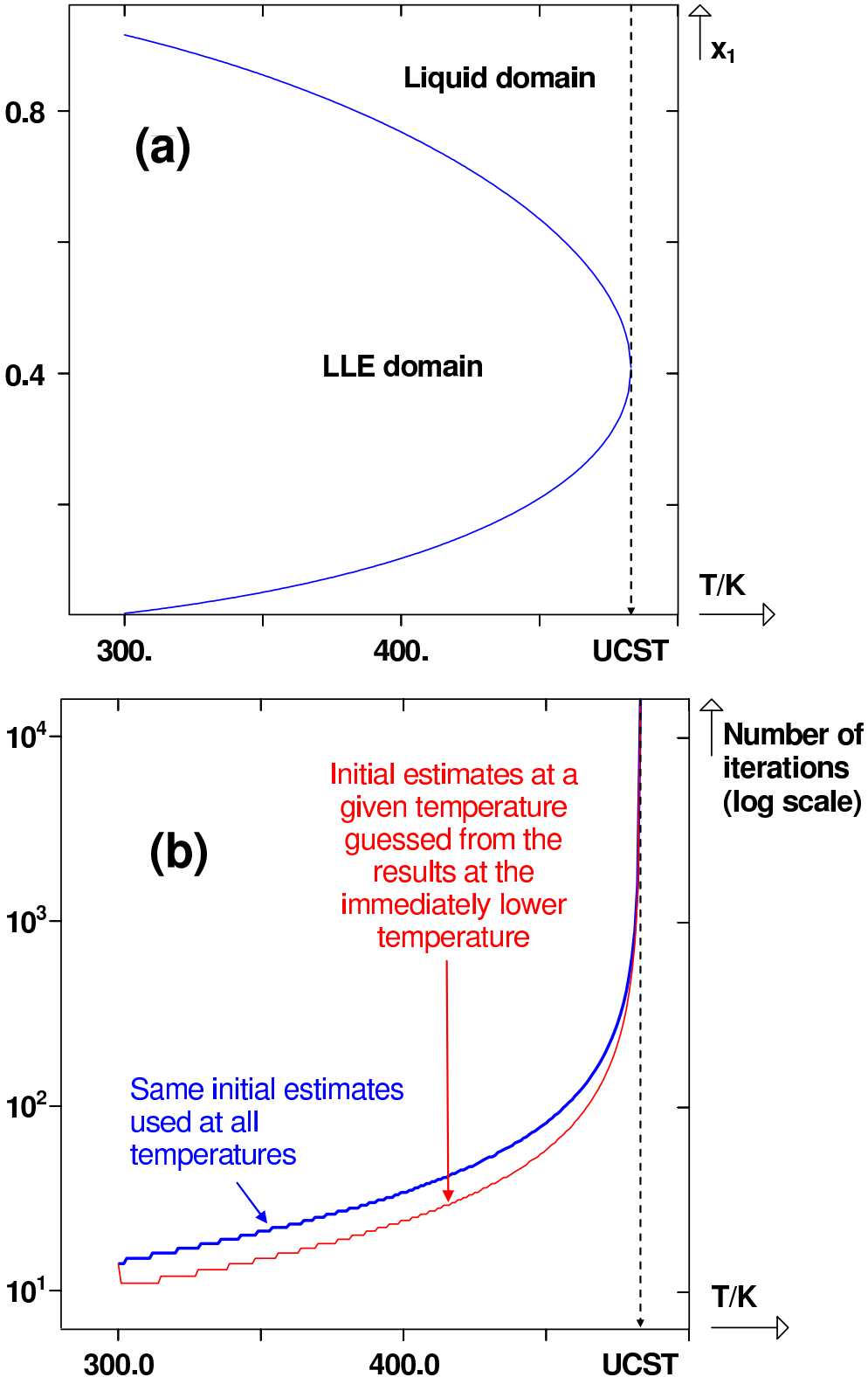

Fig. 1. (a) Composition-temperature LLE diagram calculated with Van Laar's activity coefficient model. (b) Representation of the number of iterations of the proposed LLE calculation algorithm that are necessary to reach convergence (convergence criterion: $\delta < 10^{-6}$) with respect to the temperature.

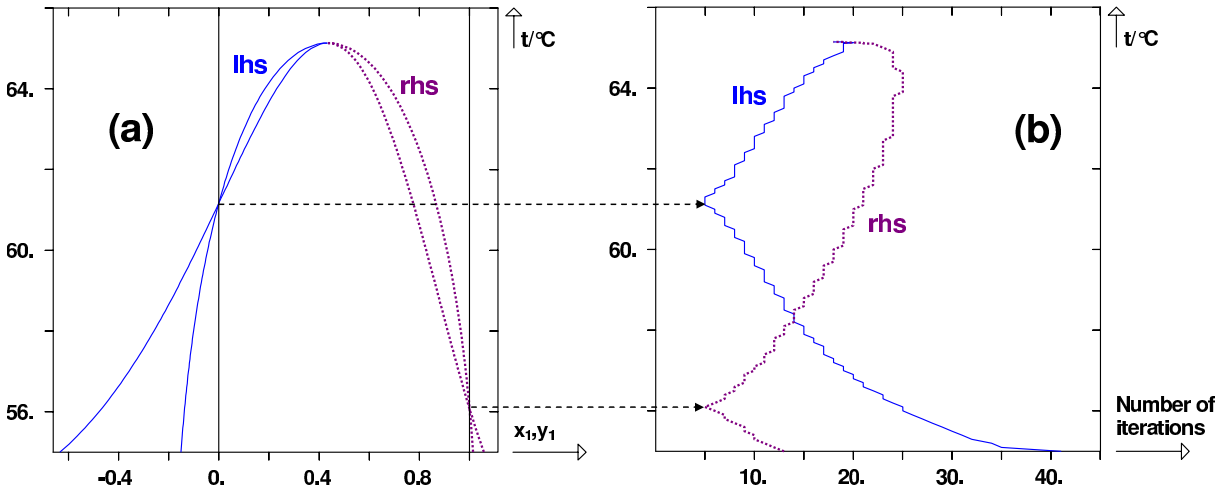

Fig. 2. (a) Isobaric phase diagram of the acetone(1) + chloroform(2) system plotted at $P = 1$ atm using the $\gamma - \varphi$ approach. (b) Representation of the number of iterations for the proposed VLE calculation algorithm that are necessary to reach convergence (convergence criterion: $\delta < 10^{-6}$) with respect to the temperature. The full and dotted lines are respectively associated with the calculation of the left hand side (*lhs*) and right hand side (*rhs*) of the phase equilibrium diagram.

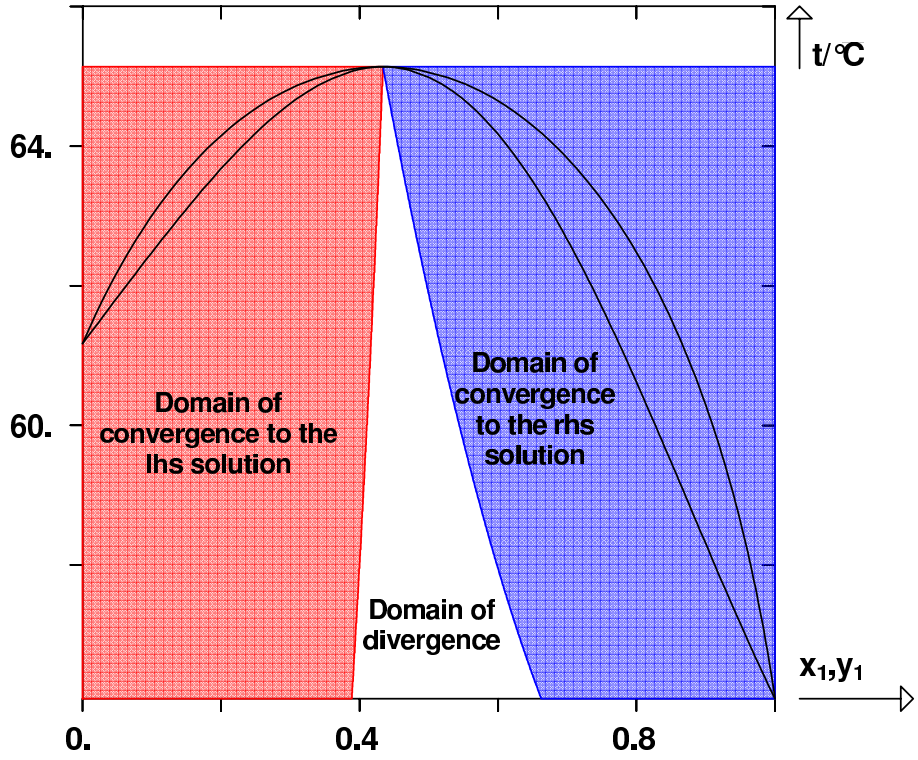

Fig. 3. Influence on the convergence of the proposed algorithm, of the chosen initial estimate for x_1.

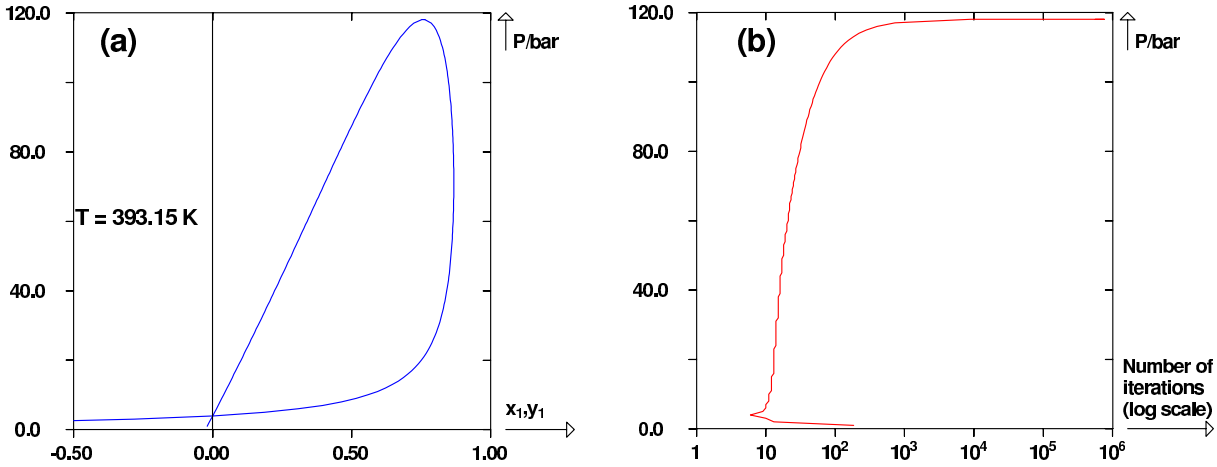

Fig. 4. (a) Isothermal phase diagram of the $CO_2(1)$ + n-hexane(2) system plotted at $T = 393.15$ K using the $\varphi - \varphi$ approach. (b) Representation of the equilibrium pressure with respect to the number of iterations that are necessary to reach convergence (convergence criterion: $\delta < 10^{-10}$).

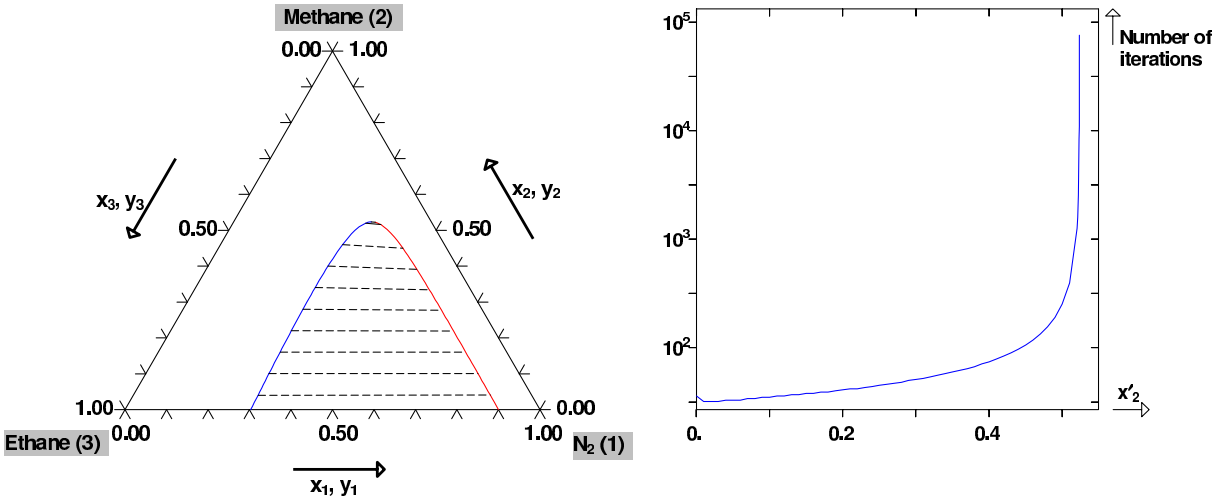

Fig. 5. *Left hand side:* fluid phase behavior of the ternary system nitrogen(1) + methane(2) + ethane(3) at 200 K and 80 bar represented in a triangular diagram. Dashed lines are tie lines. *Right hand side:* representation of the number of iterations as a function of the specified variable x_2'.

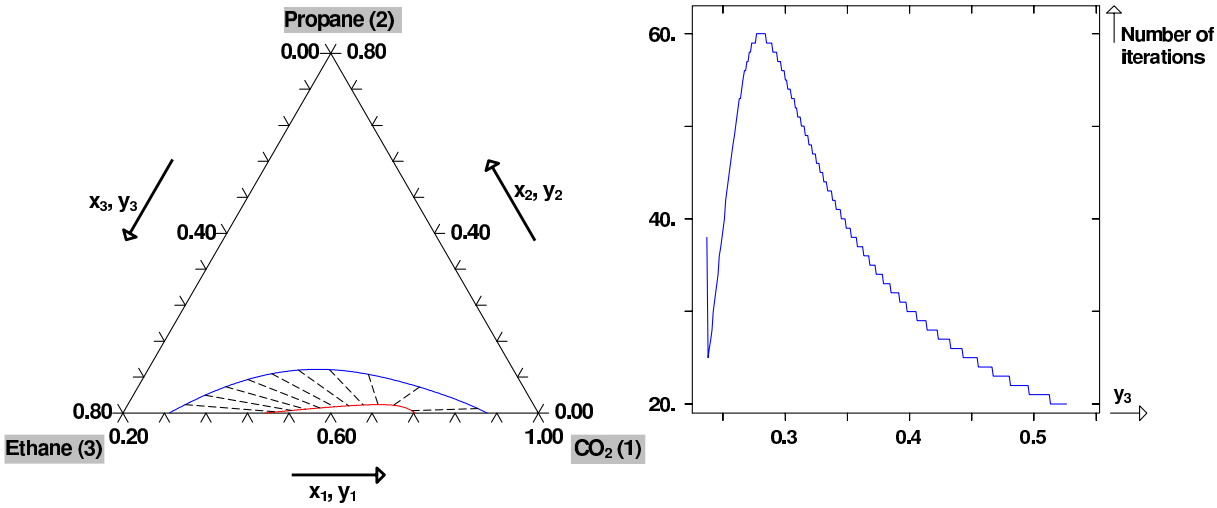

Fig. 6. *Left hand side:* fluid phase behavior of the ternary system carbon dioxide(1) + propane(2) + ethane(3) at 230 K and 11 bar represented in a triangular diagram. Dashed lines are tie lines. *Right hand side:* representation of the number of iterations as a function of the specified variable y_3.

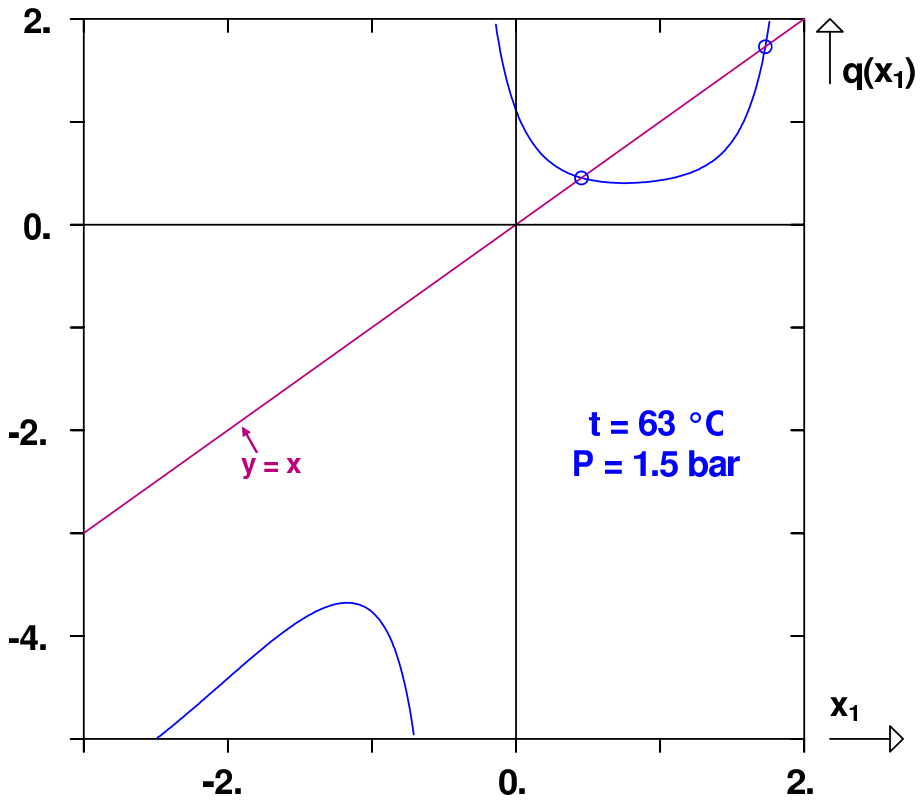

Fig. 7. Shape of the q function for a non-azeotropic system at $t = 63$ °C and $P = 1.5$ bar, having the properties presented in section 3.4 excepted $P_1^{\text{sat}} = 3$ bar and $P_2^{\text{sat}} = 1$ bar. (◯) fixed points.

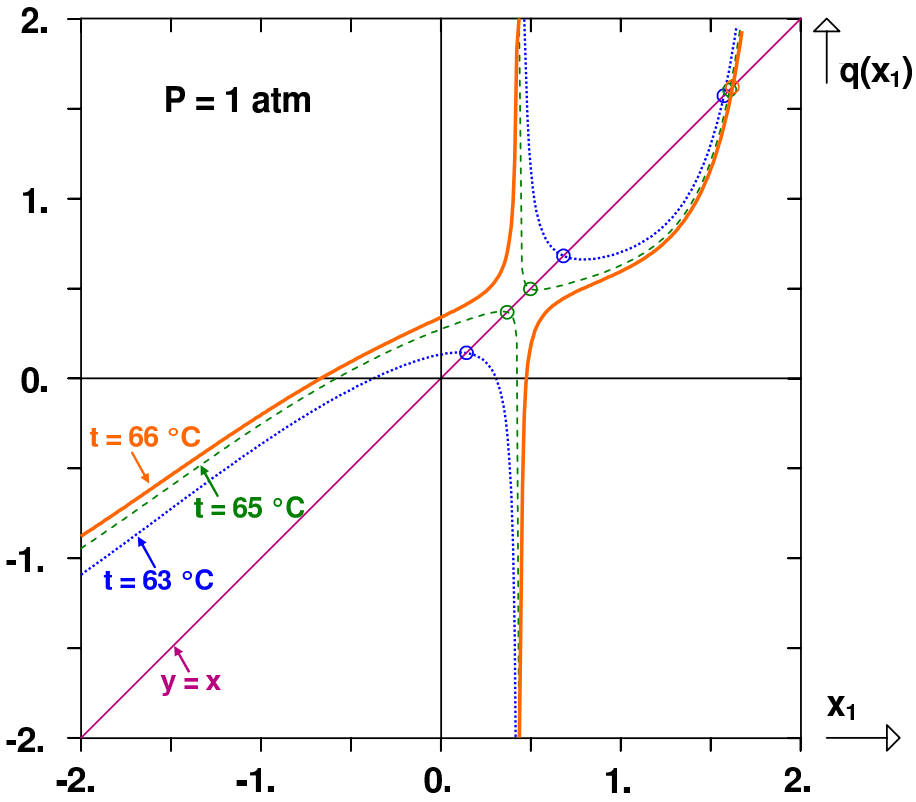

Fig. 8. Shape of the q function for an azeotropic system having the properties presented in section 3.4, at $P = 1$ atm and three different temperatures ($t = 63$ °C $< t_{\text{azeotrope}}$, $t = 65$ °C $< t_{\text{azeotrope}}$ and $t = 66$ °C $> t_{\text{azeotrope}}$). (◯) fixed points.

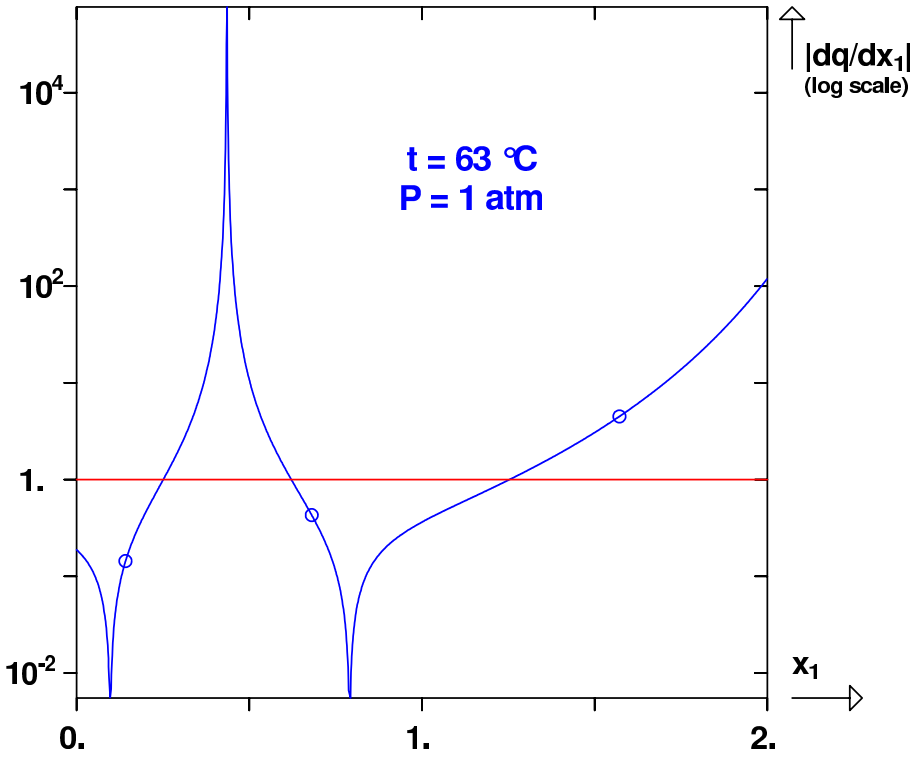

Fig. 9. Derivative of the q function for an azeotropic system at $P = 1$ atm and $t = 63\ ^\circ\mathrm{C} < t_{\mathrm{azeotrope}}$, having the properties presented in section 3.4. (◯) fixed points.

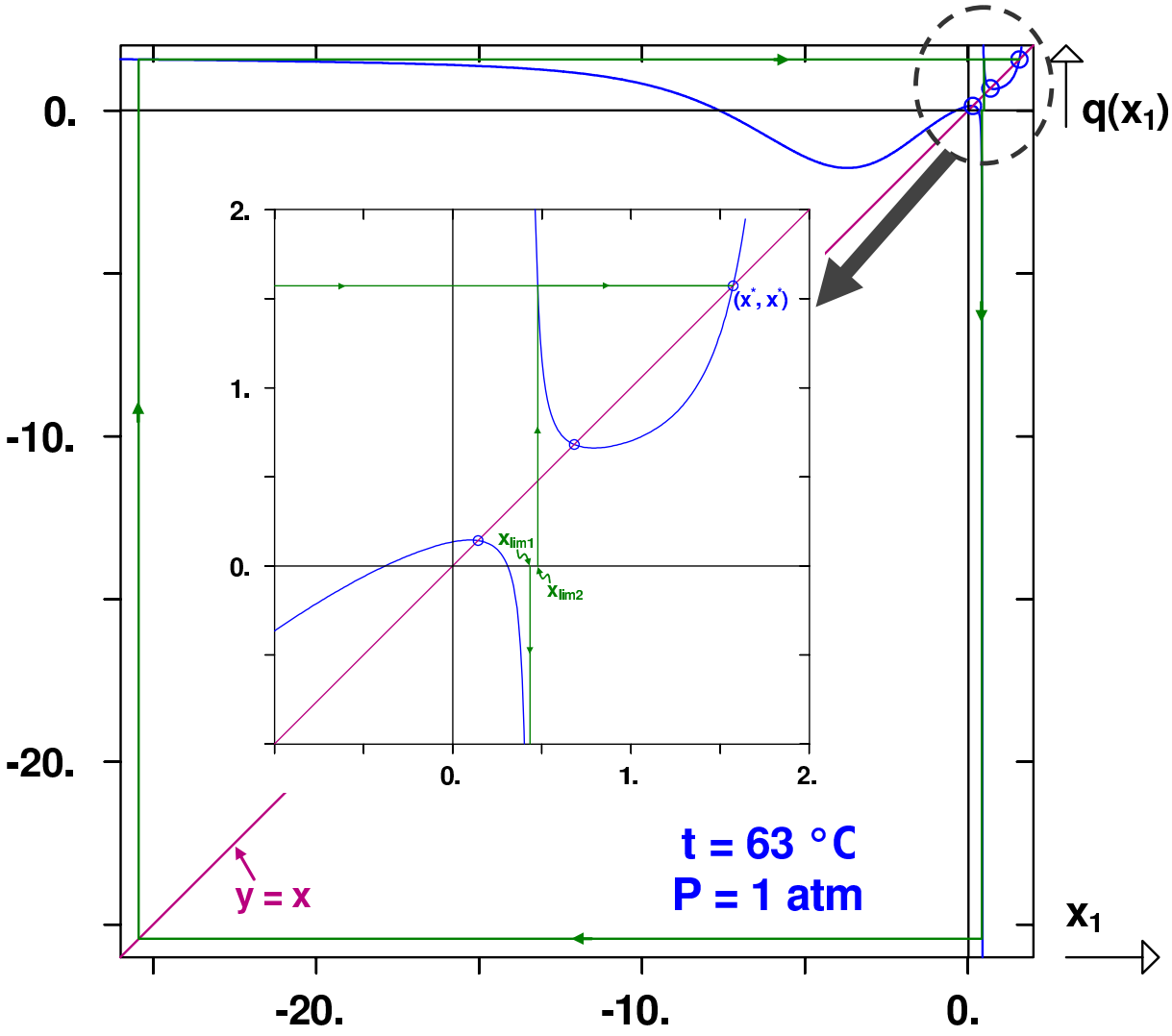

Fig. 10. Illustration that the fixed-point method initialized to $x_{\mathrm{lim},1}$ or $x_{\mathrm{lim},2}$, converges to the repulsive fixed point (x^*, x^*), for an azeotropic system at $P = 1$ atm and $t = 63\ ^\circ\mathrm{C} < t_{\mathrm{azeotrope}}$, having the properties presented in section 3.4. (◯) fixed points.